Quantum Chemistry Study of $H^+(H_2O)_8$: A Global Search for Its Isomers by the Scaled Hypersphere Search Method, and Its Thermal Behavior

Yi Luo, Satoshi Maeda, and Koichi Ohno*

Department of Chemistry, Graduate School of Science, Tohoku University, Aramaki, Aoba-ku, Sendai 980-8578, Japan

Received: June 20, 2007; In Final Form: August 12, 2007

The structures of the protonated water cluster $H^+(H_2O)_8$ have been globally explored by the scaled hypersphere search method. On the Hartree−Fock potential energy surface 174 isomers were found, among which 168 were computed to be minima at the B3LYP/6-31+G** level, and their energies were further refined at the level of MP2/6-311++G(3df,2p). The global minimum on the potential energy surface computed at the B3LYP/6-31+G** level shows a cagelike structure with the "Eigen" motif, while the lowest-free-energy isomer has a five-membered-ring structure at 170 K and a chain form at 273 K. The present results are well in line with previous experimental findings. In addition, the ADMP (atom-centered density matrix propagation) simulation indicates that the extra proton in the lowest-free-energy isomer (170 K), which has a five-membered ring and the "Zundel" feature, is often in an asymmetrical hydrogen bond.

Introduction

While extensive studies have been made to understand the behavior of water in its different forms, studies aimed at protonated water cluster, $H^+(H_2O)_n$, also have a rich and interesting history[1−29] because not only is the knowledge of these clusters of great importance for atmospheric chemistry, solution chemistry, and biological chemistry, but also such clusters are taken as a microscopic model of protonated water in the condensed phase.[10−12] One of the most basic issues in protonated water clusters is their structure, which is yet to be fully understood. The extra proton of $H^+(H_2O)_n$ is either attached to water monomer to form an "Eigen" structure (H_3O^+)[1] or is shared (equally or unequally) by water dimer to form a "Zundel" structure ($H_5O_2^+$).[2] The transformation between the Eigen and Zundel structures and their coexistence in a given $H^+(H_2O)_n$ cluster (usually $n \geq 5$) have often been discussed.[6,25] As for other cluster systems, discovering the structure of the lowest-energy isomer is also a frequent goal in the study of $H^+(H_2O)_n$. For this purpose, the global minimum, which is expected to be the most favored structure at extremely low temperatures, should first be identified. To gain insight into the structures of $H^+(H_2O)_n$ ($n = 5-8$), Jiang et al.[19] investigated the vibrational spectroscopy of these clusters at an estimated cluster temperature $T = 170 \pm 20$ K. These authors identified the isomers containing the Zundel motif at both $n = 6$ and $n = 7$, but the lowest-energy isomer of $H^+(H_2O)_8$ could not be definitely concluded due to a large number of coexisting low-lying isomers. More recent experimental work[23,26] by different groups was also done for protonated water clusters including $H^+(H_2O)_8$ at temperatures higher and lower than 170 K, but the cluster beam temperatures were difficult to be more quantitatively known. In this context, in addition to experimental efforts,[19,23,24,26] considerable theoretical calculations[5,7−9,13,14,17−20,22,27] have also been made to predict the lowest-energy isomer of $H^+(H_2O)_8$. These computations often offer some deeper insights into the structural, energetic, and dynamic aspects, which may not be obtained from experiments.

In treating any nontrivial global optimization to locate the global minimum, the principal difficulty arises from the number of minima on the potential energy surface (PES), which usually increases exponentially with the size of the system. Nonempirical methods, such as Hartree−Fock (HF), density functional theory (DFT), and second-order Møller−Plesset theory (MP2), are often used for exploring the global minimum of $H^+(H_2O)_n$ on the quantum chemical PES, and DFT and MP2 are considered to be more accurate methods to determine these cluster structures and also to estimate their energies. However, due to the computational demands for distinguishing the global minimum from a large number of topologically different but energetically similar isomers, discovering the global minimum of $H^+(H_2O)_n$ on quantum chemical PES is mostly limited to small clusters ($n < 5$)[6,25] and the larger clusters were less theoretically investigated.[5,7,9,18,19,21] An example of a full DFT calculation on $H^+(H_2O)_8$ has been demonstrated by Jiang et al.,[19] in which the computed lowest-energy isomer of $H^+(H_2O)_8$ has a five-membered-ring structure. However, they examined only a limited number of conformers of $H^+(H_2O)_8$ because of the large number of isomers to be computed. The model potential parametrized via experimental and ab initio data provides a computationally efficient alternative method with less computational consumption in comparison with ab initio approaches. There have been considerable simulation studies based on model potential. However, previous works on $H^+(H_2O)_8$ argued about the Eigen-type cage structure and the experimentally observed[19,26] Zundel-type five-membered-ring structure. For example, the KJ(H_3O^+) potential[20] predicted the Eigen-type cage structure as the global minimum but could not show the Zundel-type five-membered-ring structure. Singer's work employing OSS2 potential[30] showed the Zundel-type five-membered-ring structure and the Eigen-type cage form as a low-lying structure,[17,18] but the simulation could not present the predominance of the five-membered-ring form.[17] A computation employing MSEVB potential did show the predominance of the five-

* Corresponding author. E-mail: ohnok@qpcrkk.chem.tohoku.ac.jp.

10.1021/jp074819b CCC: $37.00
Published on Web 09/22/2007

membered-ring structure, but the MSEVB model potential calculation suggested a stable Zundel-type cage structure.[22]

The hitherto reported computations of $H^+(H_2O)_8$ could not globally search for a large number of low-lying isomers on the quantum chemical PES. Moreover, the methodological limitations in the accuracy prevent the empirical models from precisely describing the structural and energetic aspects. In this connection, our group has successfully developed a scaled hypersphere search (SHS) method,[31−33] which may automatically explore the quantum chemical PES and has been successfully applied for the system consisting of less than 8 atoms. To globally explore the isomers of larger molecular clusters (more than 20 atoms), some simplifications have been made in the SHS method.[34] The simplified SHS method has been applied for neutral water octamer,[34] and the results are in good agreement with experimental findings and Monte Carlo simulations, which stimulated us to further study a similar system, protonated water cluster. In this work, such an SHS technique has been utilized during the quantum chemical calculations of $H^+(H_2O)_8$. Considering that the entropy effect plays an important role in the stabilities of the isomers of $H^+(H_2O)_8$, the lowest-energy minima with respect to Gibbs free energies are proposed. To the best of our knowledge, this is the most thorough search for the isomers of $H^+(H_2O)_8$ on the quantum chemical potential energy surface. This work as the first example of thermodynamic simulation based on ab initio calculation shows both the predominance of the five-membered-ring structure and the Eigen-type cage form as the global minimum. Moreover, this study is in good agreement with all of the three recent experimental works.[19,23,26] In addition, the trajectory of the extra proton in a lowest-energy isomer with the Zundel motif was also demonstrated.

Computational Method

The SHS method is an uphill-walking technique to automatically explore the reaction pathway from a given equilibrium structure (EQ).[31−33] Such an exploration of reaction pathways is executed by detecting and following anharmonic downward distortions (ADDs).[31−33] This ADD following is a new concept based on a kind of principle that has arisen from deep considerations on the features of PES, and may be related to some qualitative theories such as the Bell, Evans, and Polanyi principle, the Hammond postulate, and so on. To effectively detect the ADD, a given EQ-centered hypersphere surface is introduced in the SHS technique. Such a hypersphere surface is expanded by the scaled normal coordinates q_i, which can be defined by normal coordinates Q_i and the respective eigenvalues λ_i, viz. $q_i = \lambda_i^{1/2} Q_i$. During the reaction pathway following on the scaled hypersphere surface, the conventional optimization scheme and downhill-walking technique may be utilized. By detecting and following all of the ADDs for a given EQ, the SHS method can find transition states, dissociation channels, and (or) other EQs. Such detection and following are automatically done for each newly found EQ via a one-after-another manner. Since the occurrence of a chemical reaction shows an ADD as a symptom and the lowest-energy minimum should not be out of connection with other EQs on the global potential energy surface, we believe that most of the important EQs at the low-energy region should be found by the SHS method. After the reaction pathways are traced for all the obtained EQs, the global potential energy surface may be figured. We have already made many tests for simple molecules, and many new reaction pathways as well as most of the known ones have been discovered in an automatic way. As shown in the applications to $(H_2O)_8$[34] and $H^+(H_2O)_8$, the search for known important structures as well as the global potential energy minimum of H-bond clusters has been successful.

In most previous studies on protonated water cluster, the starting structure for ab initio optimization was the model potential geometry. Such an approach can be applied only to systems where accurate model potentials are available. The SHS method can automatically search for the isomers of a given composition without using the model potential.

The ADMP (atom-centered density matrix propagation) molecular dynamics model[35,36] was used for the trajectory calculation, which was performed at 170 K utilizing the B3LYP functional and the 6-31+G** basis set. The ab initio molecular dynamics method, such as ADMP and Born−Oppenheimer molecular dynamics, describes nuclear structure classically so that the contribution due to tunneling has been ignored. However, in the current system, it is expected that such an effect is not large enough to disqualify performing trajectory analysis. Such a trajectory calculation was also previously performed for small protonated water clusters.[37] The ADMP code uses a velocity-scaling technique to control the temperature. The initial electron kinetic energy is set at zero. The simulation time step was 0.2 fs, and a valence fictitious mass of 0.1 amu was chosen. The number of total simulation steps is 1500. Except for the SHS procedures, all calculations were carried out utilizing the Gaussian 03 program.[38]

Results and Discussion

By using the SHS algorithm, 174 isomers of $H^+(H_2O)_8$ cluster were primarily located on the global PES computed at the HF/6-31G level. Among these 174 isomers, 168 ones were confirmed to be minima via geometrical reoptimization and subsequent normal-coordinate analyses at the B3LYP/6-31+G** level of theory. To gain a more accurate energy profile, single-point calculations at the MP2/6-311++G(3df,2p) level were carried out for each of the 168 isomers. The 10 lowest-energy isomers are shown in Figure 1. The computed energy relative to the lowest-energy isomers is given for each structure shown in Figure 1. For the energies reported in this figure, the electronic energies were computed at the level of MP2/6-311++G(3df,-2p), and the zero-point energy as well as free-energy corrections obtained from B3LYP/6-31+G** calculations were also added, respectively. As seen from Figure 1a, the lowest-free-energy (170 K) isomer EQ1 has the Zundel core character and a five-membered-ring structure with C_1 symmetry. This result supports the previous tentative spectral assignments.[19] The 10 lowest-free-energy (170 K) isomers include single-ring and chain structures (Figure 1a). However, the cagelike structures predominate in the 10 isomers (0 K) shown in Figure 1b. At the higher temperature $T = 273$ K, the 10 lowest-free-energy isomers are mainly chain structures (Figure 1c). According to the MP2 energy containing the zero-point-energy correction from B3LYP calculation, the cage structure EQ11 with the Eigen motif is the lowest-energy isomer (Figure 1b). Actually, EQ11 is also the lowest-energy structure according to the potential energies computed by B3LYP functional combined with 6-31+G** basis set. In this sense, the Eigen-type cage structure should be the global minimum on the PES computed at the B3LYP/6-31+G** level. This result is in line with the previous KJ(H_3O^+) model potential[4] calculation, which also suggested that the global minimum of $H^+(H_2O)_8$ has a cagelike structure similar to that of EQ11.[20] At the temperature of 273 K, the lowest-free-energy isomer shows a branched chain structure (see EQ2 in Figure 1c), which is structurally different from the

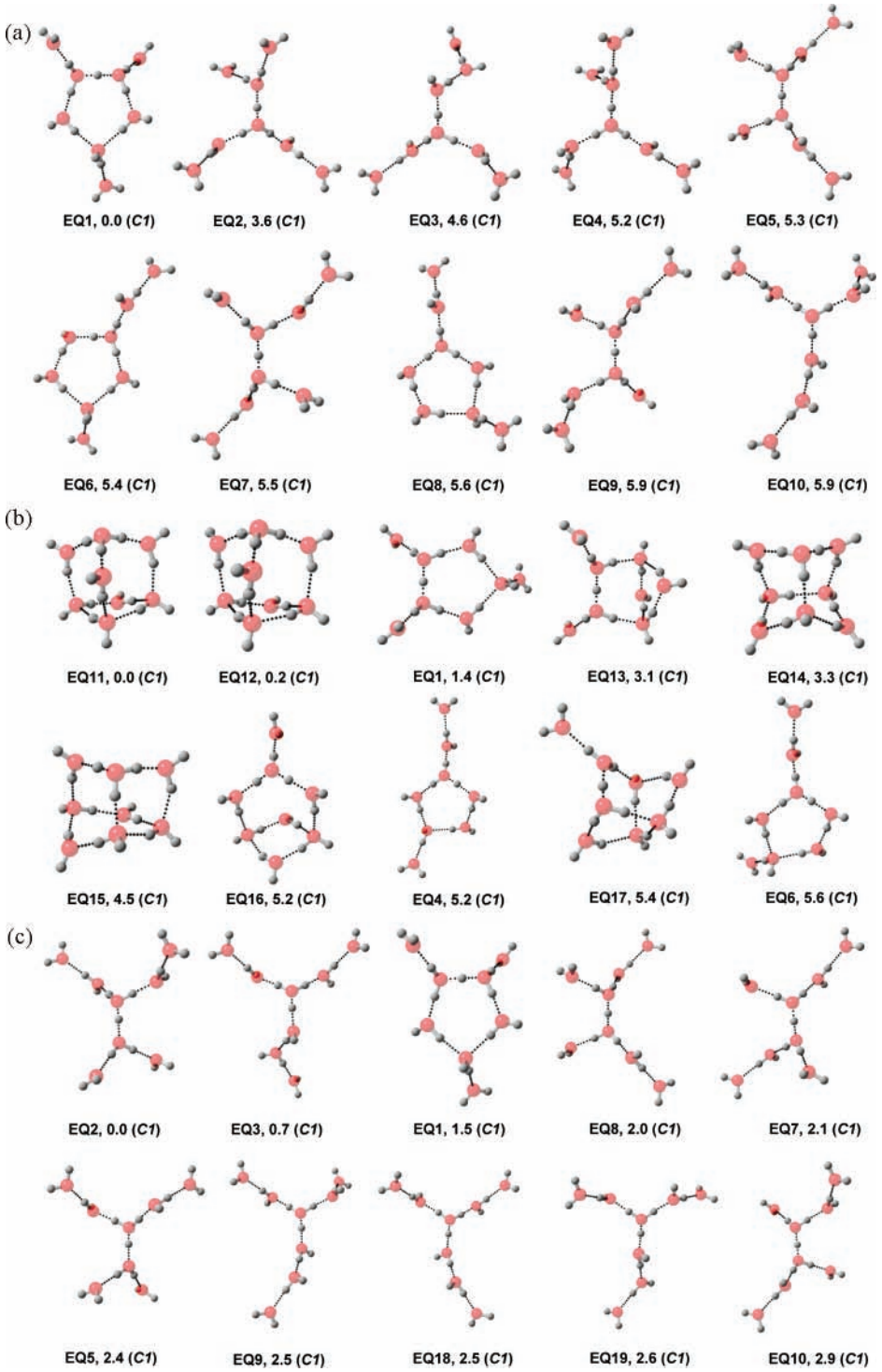

Figure 1. The 10 lowest isomers of $H^+(H_2O)_8$ cluster with respect to (a) free energy (170 K), (b) potential energy including zero-point-energy correction, and (c) free energy (273 K). The red and gray balls denote O and H atoms, respectively. The energies (in kJ/mol) are relative to lowest-energy isomers, respectively (see the text for the energy estimations). The point-group symmetry is given in parentheses.

lowest-energy isomers, EQ1 (Figure 1a) and EQ11 (Figure 1b). This is due to the fact that the structure of $H^+(H_2O)_8$ is dependent on the temperature.[19,23,26] For more detailed analysis of such a temperature dependency, a thermal population of various types of structures has been investigated (vide infra). A further structural comparison indicates that the isomers shown in Figure 1a, 1b, and 1c, respectively, do not follow the same order due to different temperatures. For example, the second-lowest-energy isomers EQ2 (Figure 1a), EQ12 (Figure 1b), and EQ3 (Figure 1c) are all structurally different. This result suggests that the entropy effect may alter the energetic ordering of the isomers, as mentioned previouslty.[18,19] The structures shown in Figure 1 also illustrate that $H^+(H_2O)_8$ favors the cagelike form at low temperature but a less compacted structure at higher temperature. Such features can be also seen from the thermodynamic population (vide infra).

To see the temperature-dependent population of the structures of $H^+(H_2O)_8$, a thermodynamic simulation has been performed, in which the 168 minima computed at the level of MP2/6-311++G(3df,2p)//B3LYP/6-31+G** were sampled. Such a thermodynamic simulation is based on the superposition method,[40] which enables one to calculate thermodynamic properties of

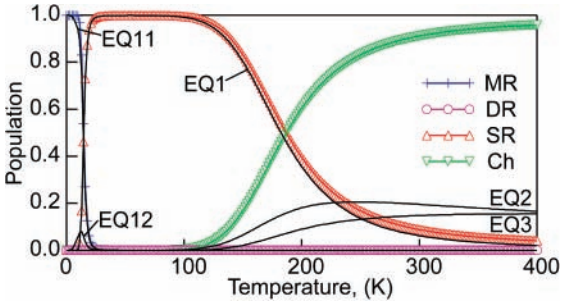

Figure 2. Temperature-dependent population of chain structures (Ch), single-ring structures (SR), double-ring structures (DR), and multi-ring structures that mainly are cagelike ones (MR). The thin lines without symbols represent the populations of several important isomers, viz. EQ1, EQ2, EQ3, EQ11, and EQ12.

clusters. The canonical probability of finding a system in a region A is[40]

$$P_A = \frac{\sum_{i\in A} Z_i(T)}{\sum_i Z_i(T)}$$

where Z_i is the partition function of the ith minimum. The Z_i can be determined by the harmonic frequency and the energy of each minimum.[41]

The energies computed at the MP2/6-311+G(3df,2p)//B3LYP/6-31+G** level and the results of B3LYP/6-31+G** frequency calculations were used for this simulation. All of the 168 minima can be structurally grouped into four types of forms, viz. chain structures, single-ring structures, double-ring structures, and multi-ring structures that mainly are cage forms. The probability population curves of the four types of structures against the temperature are shown in Figure 2. In addition, the temperature-dependent populations of some important isomers, viz. EQ1, EQ2, EQ3, EQ11, and EQ12, are also included in this figure. As seen from Figure 2, the chain form predominates over the single-ring structure at $T > 190$ K, while the dominant population of single-ring structure appears at temperatures lower than about 190 K. At $T \approx 170$ K, both the single-ring and the chain structures contribute to the population, and the former has larger probability. EQ1, which is computed to be the lowest-energy isomer at 170 K (Figure 1a), has a five-membered ring and therefore follows the distribution trend of the single-ring structures. This result is in line with previous work,[19] in which the authors claimed that EQ1 is one of the lowest-energy isomers of $H^+(H_2O)_8$ at $T \approx 170$ K and also addressed that many isomers may coexist with EQ1. The population (Figure 2) at $T \approx 170$ K indicates that those coexisting isomers mostly have a chain form. In a previous experimental work, the spectrum of Ar-attached $H^+(H_2O)_8$ was clearly dominated by the Zundel-based structure EQ1 at low temperature.[26] In this computational study, the population at the temperatures of 20−130 K (Figure 2), where the single-ring structure has more than 95% probability population and the EQ1 also predominates, agrees exceptionally well with the experimental observation.[26]

The harmonic spectra of EQ1 has been reported previously.[18,19,26] Especially the harmonic IR spectra of EQ1 computed by Singer et al. showed a strong O−H−O proton oscillation peak (at ~1000 cm^{-1}),[18] which corresponds well to the most important characteristic of the experimentally observed spectra for EQ1.[26] In the same experimental work,[26] the authors found that Ar-tagged $H^+(H_2O)_8$ was clearly dominated by the EQ1 structure. Our calculation also showed the predominance of EQ1 (Figure 2), which together with previous harmonic IR spectra[18] strongly supports the experimental observation.[26] Future dynamics-based anharmonic analysis[39] may make the spectra closer to experimental ones. The population of cagelike structure predominates at the temperature of a few kelvin but drops rapidly into near zero at $T \approx 20$ K and remains near zero population at the higher temperatures considered (Figure 2). The same is true for EQ11, which is found to be the lowest-energy isomer (Figure 1b) at 0 K. The result that the cagelike structure, such as EQ11, dominates the population at $T < 20$ K (Figure 2) is in agreement with the previous model potential calculation by Wales et al.[20] and Jordan et al.[22] The former work[20] on the basis of the KJ(H_3O^+) model potential[4] predicted a cagelike structure similar to EQ11 as the global minimum of $H^+(H_2O)_8$, and the later one[22] on the basis of the multistate empirical valence-bond (MSEVB) model[10] suggested a dominant population of cage form at such a low-temperature region. At the higher temperatures (190−400 K) considered (Figure 2), the chain structure is the most populated form. Such a situation is comparable to the results from Monte Carlo simulation,[17,22] by which the temperature for the dominant population of chain structure is proposed to be above 160 K. As seen from Figure 2, the chain structure predominates at $T > 190$ K and has a population of more than 95% at $T > 290$ K. This result is consistent with the previous experimental work reported by Mikami et al.,[23] in which the authors observed the spectrum of the terminal water molecule of $H^+(H_2O)_8$ with a chain structure at temperatures much higher than 170 K.

As suggested by the population curves of the four kinds of structures (Figure 2), the cage-structure-involved isomer has nearly zero population at $T > 20$ K, while the chain structure has a population at $T \approx 100$ K and predominates at the higher temperatures (>190 K) considered. The single-ring structure has the exclusive population at the temperatures of 20−130 K. However, the double-ring structure has no significant population at the selected temperature although many double-ring structures were located to be minima at the B3LYP/6-31+G** level of theory. We have also made test calculations on the basis-set superposition error (BSSE) and considered the anharmonic effects in the previous paper concerning the $(H_2O)_8$ cluster.[34] Such errors were significant in absolute value and affected energies of all structures in the same direction. We expected that such errors might shift transition temperatures by several tens of kelvin,[34] which is acceptable for qualitative discussion. The present treatment for the current analogous system may also provide qualitative understanding of temperature effects on the cluster structures, since our results reproduced well qualitative features of previous experimental results as well as Monte Carlo simulations for $(H_2O)_8$ and $H^+(H_2O)_8$. Although care should be taken due to the method errors, the current population analysis suggests the temperature region where the EQ1 dominates. Such information may be helpful for estimating the cluster beam temperature in the previous experiment, which showed the predominance of the EQ1 structure.[26]

As described above, by using the SHS method, the present simulation result is consistent with experimental observations reported by different groups, and the Eigen-type cage structure predicted by model potential was also located as the global minimum on PES. Such agreements suggest that the SHS method may be used to search for the isomers of a given H-bond cluster system without model potential, as seen from its successful applications to $H^+(H_2O)_8$ and $(H_2O)_8$.[34]

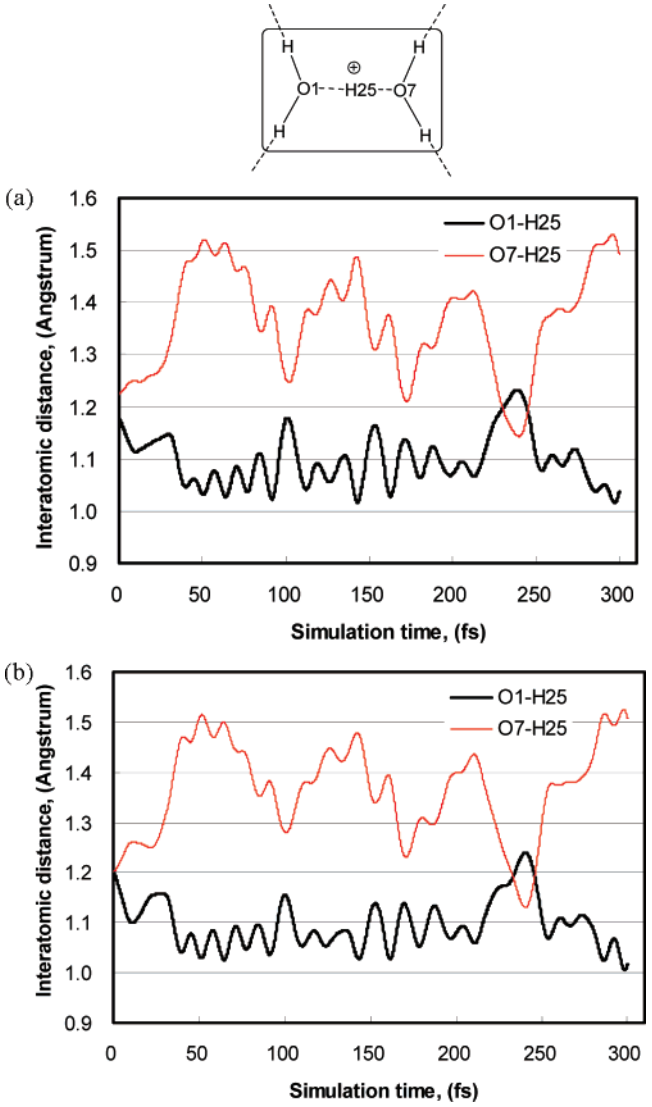

Figure 3. ADMP simulation results. The initial structures of the simulations are based on the EQ1: (a) the proton H25 of the initial structure (optimized EQ1 at B3LYP/6-31+G** level) is in an asymmetrical hydrogen bond and (b) the proton H25 of the initial structure is set to be in a symmetrical hydrogen bond. The Zundel core structure of EQ1 is schematically shown above for atom labeling. The black lines show the change of O1−H25 distance, and the red lines show the change of O7−H25 distance.

The previous static computations argued whether the extra proton of the Zundel-core-embedded structure of the protonated water clusters is in a symmetrical hydrogen bond.[18,19] Such a situation caused us to wonder the trajectory of the extra proton in EQ1 with the Zundel motif. For this purpose, the ADMP simulations were performed at 170 K on the basis of the EQ1 structure. The structure of EQ1 and the temperature of 170 K were chosen because not only is EQ1 computed to be the lowest-energy isomer with respect to the free energy (170 K) in this study but also the observed spectra of $H^+(H_2O)_8$ at $T \approx 170$ K were tentatively assigned to EQ1.[19] The ADMP simulation results are shown in Figure 3. The variation of O1−H25 and O7−H25 distances (see Figure 3) reflects the trajectory of the extra proton (H25). One simulation was initiated from the EQ1 structure, in which the excess proton is not exactly equidistant from its two oxygen neighbors (1.180 and 1.224 Å, respectively). As seen from Figure 3a, there are two cross-points at 230 and 245 fs, respectively, which appear within a rather short time interval (15 fs). This result suggests that the extra proton is mostly in an asymmetrical hydrogen bond and closer to the O1 atom at the temperature of about 170 K. To see whether such a trajectory is due to the initial unequal distances between the proton (H25) and its two neighboring oxygen atoms (O1 and O7), a further ADMP simulation was carried out. The further simulation started with an adjusted EQ1 structure with the extra proton situated at the midpoint of its two oxygen neighbors. The obtained trajectory (Figure 3b), which is similar to that in Figure 3a, also suggests that the interactions of the extra proton with its two oxygen neighbors are mostly unequal, which is in line with the previous result reported by Singer and his co-workers.[18]

Conclusions

In this study, the scaled hypersphere search method has been utilized to globally explore the structures of $H^+(H_2O)_8$. On the HF potential energy surface 174 isomers of $H^+(H_2O)_8$ were found, and 168 ones were located to be minima at the B3LYP/6-31+G** level of theory. The lowest-free-energy isomer of the $H^+(H_2O)_8$ at the temperature of 170 K has a five-membered-ring structure with the Zundel core character. However, a cagelike structure with the Eigen character has been computed to be the global minimum on the B3LYP potential energy surface (0 K), and a chain structure has been found to be the lowest-free-energy isomer at the higher temperature $T = 273$ K. Furthermore, the thermodynamic simulation shows that the isomers with a single-ring structure dominate the probability (with a population of more than 95%) at the temperatures of 20−130 K. However, the population at higher temperature considered ($T > 190$ K) is dominated by a chain structure. The present study is in line with previous experimental works reported by different groups. In addition, for the lowest-free-energy (170 K) isomer EQ1 with the Zundel motif, the DFT-based trajectory calculations show that the extra proton often unequally interacts with its two neighboring oxygen atoms at the temperature considered (170 K).

Acknowledgment. This work was partly supported by the Grants-in-Aid for Scientific Research (No. 17655001) from the Ministry of Education, Science, Sports, and Culture, and the Grant-in-Aid for the COE project, Giant Molecules and Complex System, 2004. Y.L. acknowledges the Japan Society for the Promotion of Science (JSPS) for research fellowship. S.M. is supported by a Research Fellowship of JSPS for Young Scientists. The authors also thank the Tohoku University Information Synergy Center, parallel computing system, for part of the computational time. We send many thanks to Dr. X. Yang for helpful discussions.

Supporting Information Available: List giving the optimized Cartesian coordinates of the 168 isomers and their relative energies. This material is available free of charge via the Internet at http://pubs.acs.org.

References and Notes

(1) Eigen, M. *Angew. Chem., Int. Ed. Engl.* **1964**, *3*, 1.
(2) Zundel, G. In *The Hydrogen Bond—Recent Developments in Theory and Experiments. II. Structure and Spectroscopy*; Schuster, P., Zundel, G., Sandorfy, C., Eds.; North-Holland: Amsterdam, 1976; pp 683−766.
(3) Yeh, L. I.; Okumura, M.; Myers, J. D.; Price, J. M.; Lee, Y. T. *J. Chem. Phys.* **1989**, *91*, 7319.
(4) Kozack, R. E.; Jordan, P. C. *J. Chem. Phys.* **1992**, *96*, 3131.
(5) Termath, V.; Sauer, J. *Mol. Phys.* **1997**, *91*, 963.
(6) Kochanski, E.; Kelterbaum, R.; Klein, S.; Rohmer, M. M.; Rahmouni, A. *Adv. Quantum Chem.* **1997**, *28*, 273, and the references therein.

(7) Wei, D.; Salahub, D. R. *J. Chem. Phys.* **1997**, *106*, 6086.
(8) McDonald, S.; Ojamäe, L.; Singer, S. J. *J. Phys. Chem. A* **1998**, *102*, 2824.
(9) Cheng, H. P. *J. Phys. Chem. A* **1998**, *102*, 6201.
(10) Schmitt, U. W.; Voth, G. A. *J. Phys. Chem. B* **1998**, *102*, 5547.
(11) Vuilleumier, R.; Borgis, D. *J. Phys. Chem. B* **1998**, *102*, 4261.
(12) Marx, D.; Tuckerman, M. E.; Hutter, J.; Parrinello, M. *Science* **1999**, *397*, 601.
(13) Shevkunov, S. V.; Vegiri, A. *J. Chem. Phys.* **1999**, *111*, 9303.
(14) Hodges, M. P.; Stone, A. J. *J. Chem. Phys.* **1999**, *110*, 6766.
(15) Schmitt, U. M.; Voth, G. A. *J. Chem. Phys.* **1999**, *111*, 9361.
(16) Geissler, P. L.; Dellago, C.; Chaandler, D.; Hutter, J.; Parrinello, M. *Chem. Phys. Lett.* **2000**, *321*, 225.
(17) Singer, S. J.; Mcdonald, S.; Ojamäe, L. *J. Chem. Phys.* **2000**, *112*, 710.
(18) Ciobanu, C. V.; Ojamäe, L.; Shavitt, I.; Singer, S. J. *J. Chem. Phys.* **2000**, *113*, 5321.
(19) Jiang, J. C.; Wang, Y. S.; Chang, H. C.; Lin, S. H.; Lee, Y. T.; Niedner-Schatteburg, G.; Chang, H. C. *J. Am. Chem. Soc.* **2000**, *122*, 1398.
(20) Hodges, M. P.; Wales, D. J. *Chem. Phys. Lett.* **2000**, *324*, 279.
(21) Khan, A. *Chem. Phys. Lett.* **2000**, *319*, 440.
(22) Christie, R. A.; Jordan, K. D. *J. Phys. Chem. B* **2002**, *106*, 8376.
(23) Miyazaki, M.; Fujii, A.; Ebata, T.; Mikami, N. *Science* **2004**, *304*, 1134.
(24) Shin, J. W.; Hammer, N. I.; Diken, E. G.; Johnson, M. A.; Walters, R. S.; Jaeger, T. D.; Duncan, M. A.; Christie, R. A.; Jordan, K. D. *Science* **2004**, *304*, 1137.
(25) Chang, H. C.; Wu, C. C.; Kuo, J. L. *Int. Rev. Phys. Chem.* **2005**, *24*, 553, and references therein.
(26) Headrick, J. M.; Diken, E. G.; Walters, R. S.; Hammer, N. I.; Christie, R. A.; Cui, J.; Myshakin, E. M.; Duncan, M. A.; Johnson, M. A.; Jordan, K. D. *Science* **2005**, *308*, 1765.
(27) Kuo, J. L.; Klein, M. L. *J. Chem. Phys.* **2005**, *122*, 024516.
(28) Kuo, J. L. *J. Phys. Conf. Ser.* **2006**, *28*, 87.
(29) McDonald, S.; Ojamäe, L.; Singer, S. J. *J. Phys. Chem. A* **1998**, *102*, 2824.
(30) Ojamäe, L.; Shavitt, I.; Singer, S. J. *J. Chem. Phys.* **1998**, *109*, 5547.
(31) Ohno, K.; Maeda, S. *Chem. Phys. Lett.* **2004**, *384*, 277.
(32) Maeda, S.; Ohno, K. *J. Phys. Chem. A* **2005**, *109*, 5742.
(33) Ohno, K.; Maeda, S. *J. Phys. Chem. A* **2006**, *110*, 8933.
(34) Maeda, S.; Ohno, K. *J. Phys. Chem. A* **2007**, *111*, 4527.
(35) Schlegel, H. B.; Millam, J. M.; Iyengar, S. S.; Voth, G. A.; Daniels, A. D.; Scuseria, G. E.; Frisch, M. J. *J. Chem. Phys.* **2001**, *114*, 9758.
(36) Schlegel, H. B.; Iyengar, S. S.; Li, X.; Millam, J. M.; Voth, G. A.; Scuseria, G. E.; Frisch, M. J. *J. Chem. Phys.* **2002**, *117*, 8694.
(37) Wei, D.; Salahub, D. R. *J. Chem. Phys.* **1997**, *106*, 6086.
(38) Frisch, M. J.; Trucks, G. W.; Schlegel, H. B.; Scuseria, G. E.; Robb, M. A.; Cheeseman, J. R.; Montgomery, J. A., Jr.; Vreven, T.; Kudin, K. N.; Burant, J. C.; Millam, J. M.; Iyengar, S. S.; Tomasi, J.; Barone, V.; Mennucci, B.; Cossi, M.; Scalmani, G.; Rega, N.; Petersson, G. A.; Nakatsuji, H.; Hada, M.; Ehara, M.; Toyota, K.; Fukuda, R.; Hasegawa, J.; Ishida, M.; Nakajima, T.; Honda, Y.; Kitao, O.; Nakai, H.; Klene, M.; Li, X.; Knox, J. E.; Hratchian, H. P.; Cross, J. B.; Bakken, V.; Adamo, C.; Jaramillo, J.; Gomperts, R.; Stratmann, R. E.; Yazyev, O.; Austin, A. J.; Cammi, R.; Pomelli, C.; Ochterski, J. W.; Ayala, P. Y.; Morokuma, K.; Voth, G. A.; Salvador, P.; Dannenberg, J. J.; Zakrzewski, V. G.; Dapprich, S.; Daniels, A. D.; Strain, M. C.; Farkas, O.; Malick, D. K.; Rabuck, A. D.; Raghavachari, K.; Foresman, J. B.; Ortiz, J. V.; Cui, Q.; Baboul, A. G.; Clifford, S.; Cioslowski, J.; Stefanov, B. B.; Liu, G.; Liashenko, A.; Piskorz, P.; Komaromi, I.; Martin, R. L.; Fox, D. J.; Keith, T.; Al-Laham, M. A.; Peng, C. Y.; Nanayakkara, A.; Challacombe, M.; Gill, P. M. W.; Johnson, B.; Chen, W.; Wong, M. W.; Gonzalez, C.; Pople, J. A. *Gaussian 03*, revision D.02; Gaussian, Inc.: Wallingford, CT, 2004.
(39) For examples, see: (a) Kuo, I.-F. W.; Tobias, D. J. *J. Phys. Chem. A* **2002**, *106*, 10969. (b) Greathouse, J. A.; Cygan, R. T.; Simmons, B. A. *J. Phys. Chem. B* **2006**, *110*, 6428.
(40) Wales, D. J.; Doye, J. P. K.; Miller, M. A.; Mortenson, P. N.; Walsh, T. R. *Adv. Chem. Phys.* **2000**, *115*, 1.
(41) Jensen, F. In *Introduction to Computational Chemistry*; John Wiley & Sons Ltd.: Chichester, U.K., 1999.